

CD146 bound to LCK promotes TCR signaling and anti-tumor immune response in mice

Hongxia Duan^{1,#}, Lin Jing^{1,2,#}, Xiaoqing Jiang¹, Yanbin Ma^{1,2}, Daji Wang^{1,2}, Jianquan Xiang¹, Xuehui Chen¹, Zhenzhen Wu¹, Huiwen Yan¹, Junying Jia³, Zheng Liu¹, Jing Feng¹, Mingzhao Zhu^{2,4,*}, Xiyun Yan^{1,2,5,*}

¹Key Laboratory of Protein and Peptide Pharmaceutical, Institute of Biophysics, Chinese Academy of Sciences, Beijing 100101, China

² College of Life Sciences, University of Chinese Academy of Sciences, Beijing 100049, China

³ Core Facility for Protein Research, Institute of Biophysics, Chinese Academy of Sciences, Beijing 100101, China

⁴ Key Laboratory of Infection and Immunity, Institute of Biophysics, Chinese Academy of Sciences, Beijing 100101, China

⁵ Joint Laboratory of Nanozymes in Zhengzhou University, School of Basic Medical Sciences, Zhengzhou University, Zhengzhou 450001, China.

#These authors contributed equally to this work.

*Correspondence:

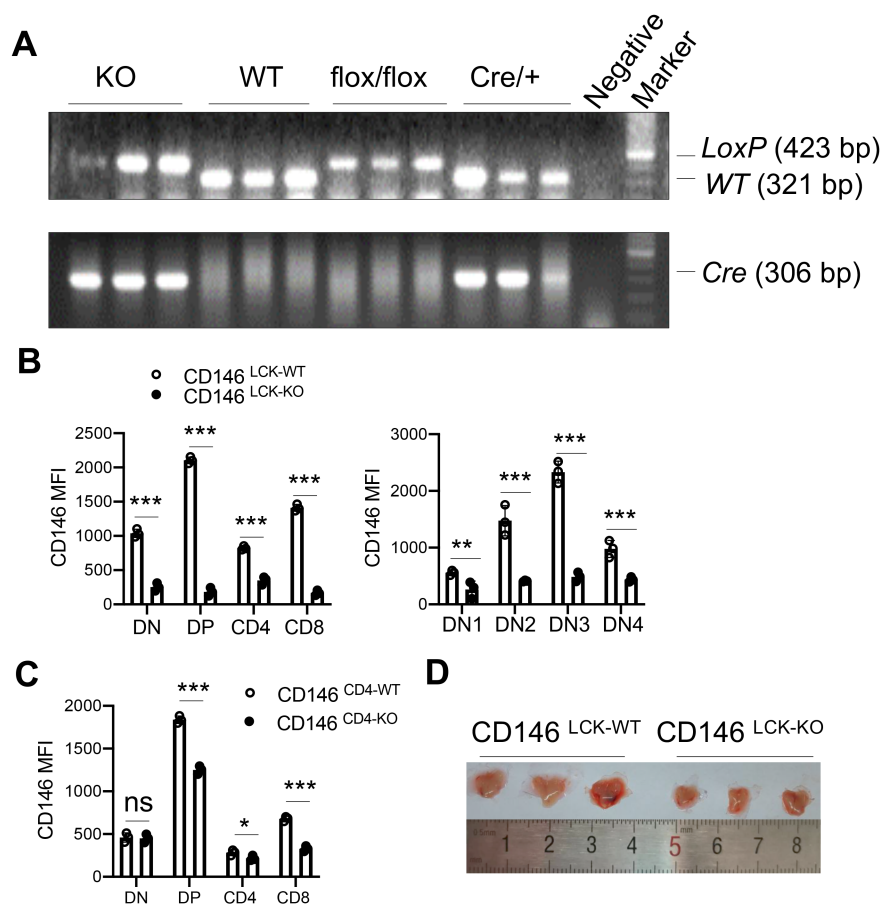
Mingzhao Zhu, E-mail: zhumz@ibp.ac.cn, Tel.: +86 10 64888775. Fax: +86 10 64871293;

Xiyun Yan, E-mail: yanxy@ibp.ac.cn, Tel.: +86 10 64888583. Fax: +86 10 64888584.

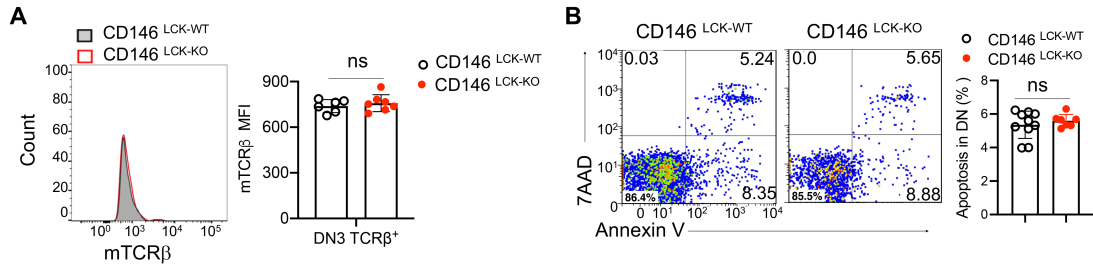
Running title: CD146 mediates TCR signaling by binding to LCK

Key words: CD146, LCK activation, TCR signaling, T cell activation

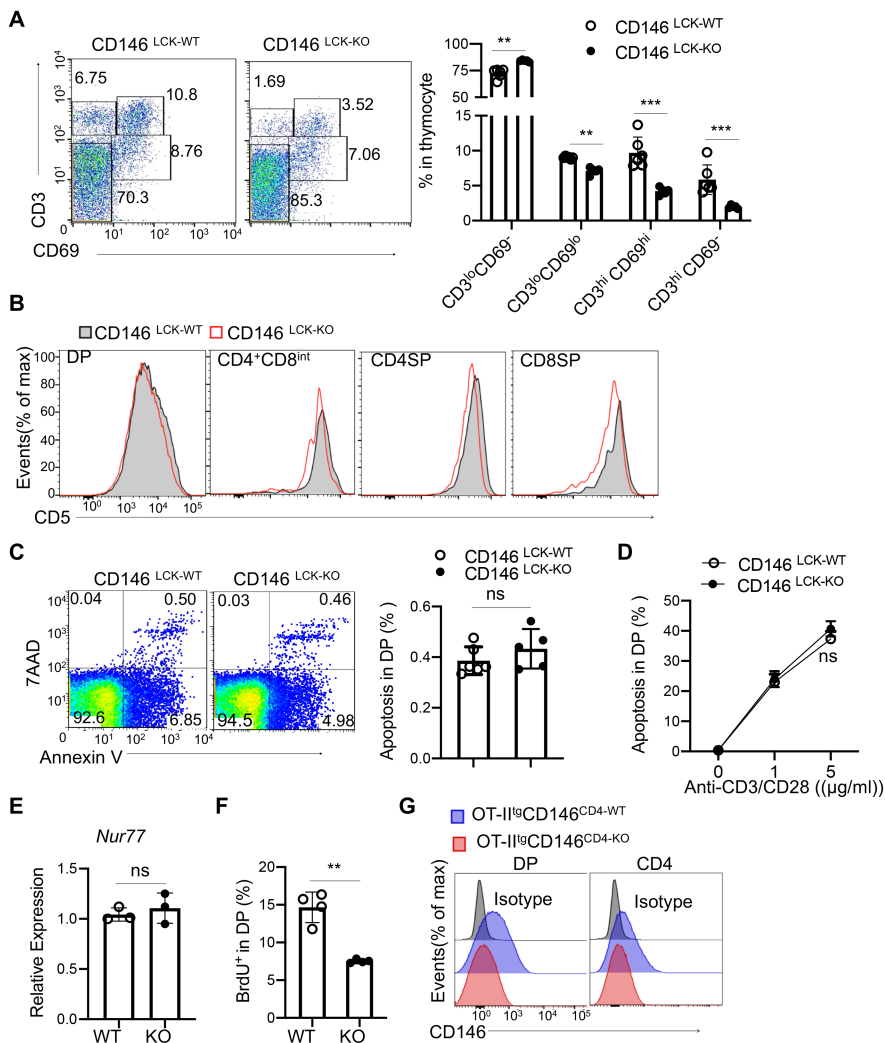
Supplementary Figures



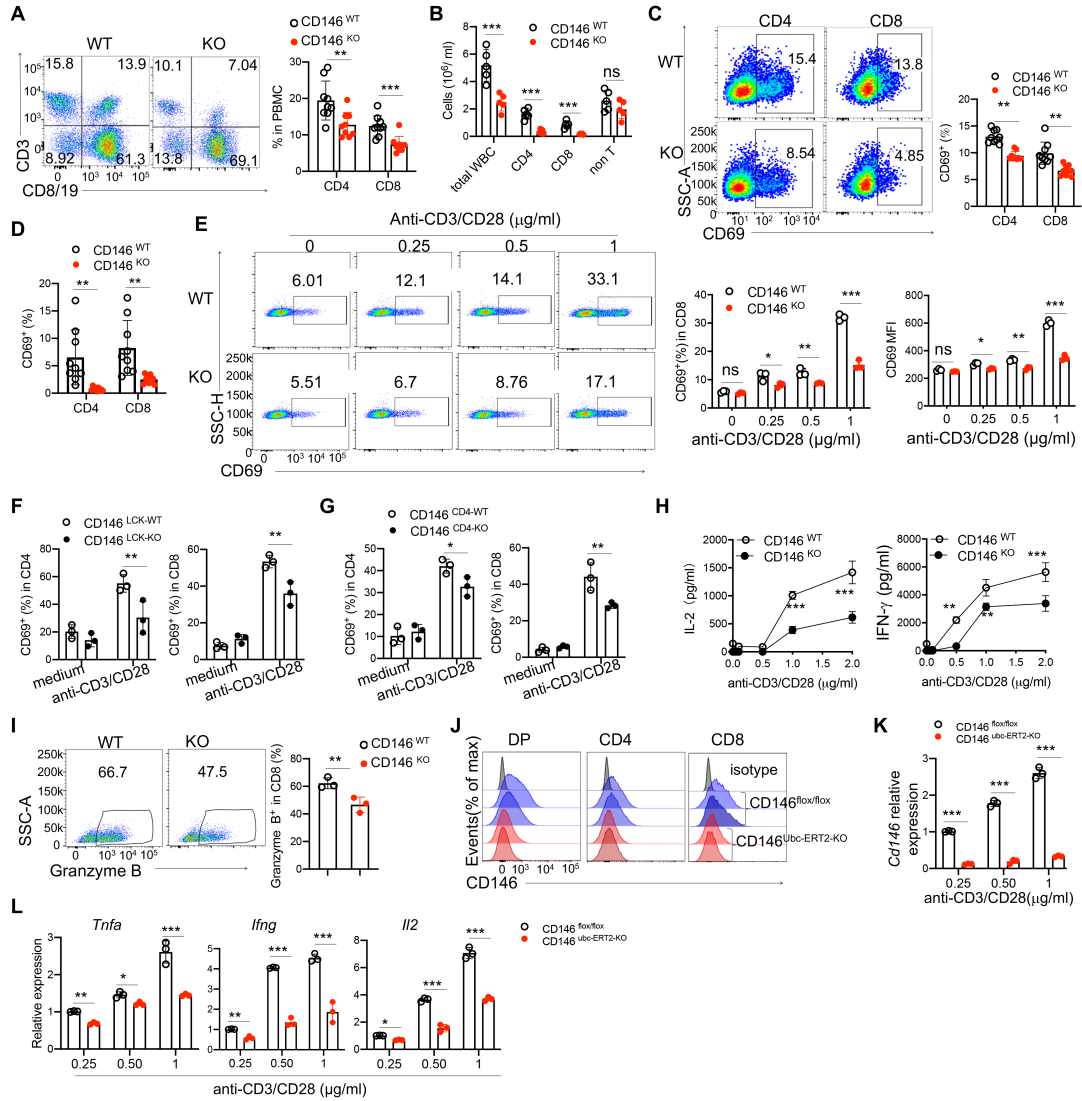
Supplementary Fig 1. Analysis of CD146 conditional knockout mice. (A) PCR analysis of genotypes of mice (representative of $n = 3$). **(B, C)** MFI of CD146 on DN1-DN4, DP, CD4, and CD8 subpopulations of thymocytes from conditional knockout mice ($n = 3$). **(D)** Thymuses from WT mice and conditional knockout mice (representative of $n = 3$). Each symbol represents an individual mouse. One-way ANOVA followed by Bonferroni's correction was performed. Data are shown as mean \pm SEM. * $p < 0.05$, ** $p < 0.01$.



Supplementary Fig. 2. CD146 is required for β selection. (A) Surface staining of membrane TCR β (m TCR β) in DN3 cells. Right, mTCR β MFI in DN3 TCR β^+ cells (n = 6 for WT or 7 for KO). (B) Apoptosis of DN cells from CD146^{LCK-WT} and CD146^{LCK-KO} mice. Right, percentages of apoptosis (n = 10 for WT or 7 for KO). Each symbol represents an individual mouse. Two-tailed *t*-test was performed. n.s, not significant.

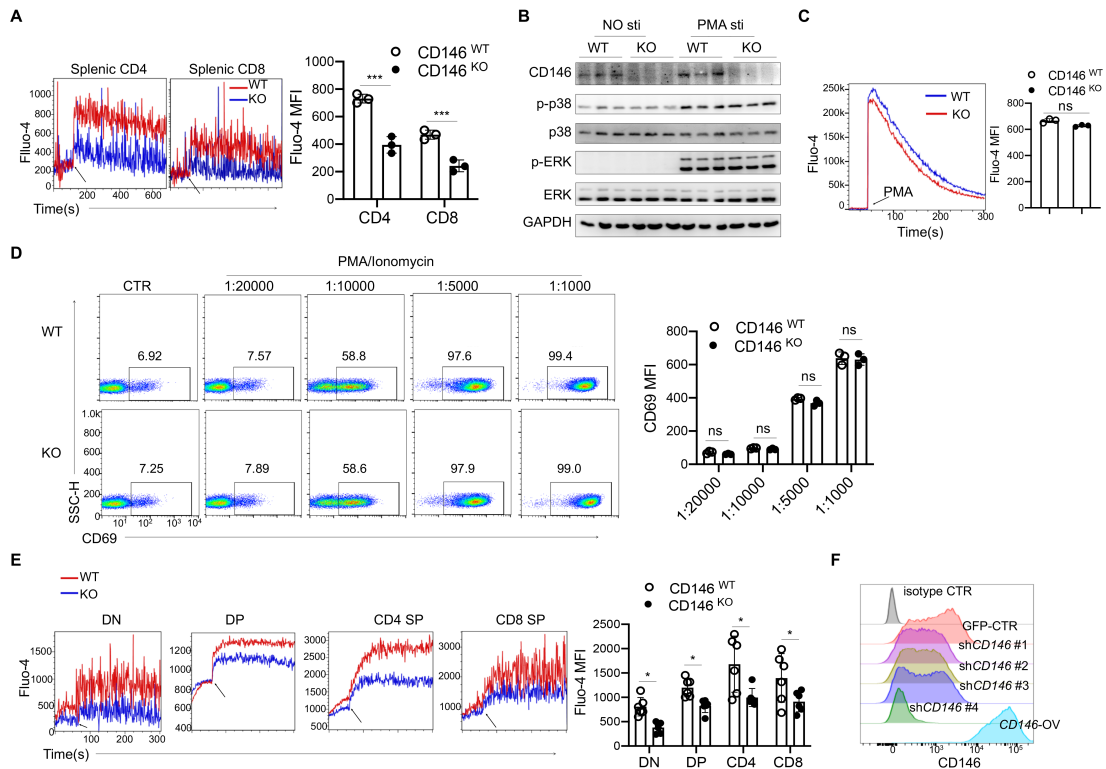


Supplementary Fig 3. CD146 is required for positive selection. (A) Surface staining of CD3 and CD69 on thymocytes (Left) from CD146^{LCK-WT} and CD146^{LCK-KO} mice; numbers adjacent to outlined areas indicate percent cells in each gate. Right, percentages of CD3^{lo}CD69⁻, CD3^{lo}CD69^{lo}, CD3^{hi}CD69⁻, and CD3^{hi}CD69^{hi} subpopulations in 10 thymuses (n = 10). (B) Surface staining of CD5 from gated CD4⁺CD8^{int}, DP, and SP cells of CD146^{LCK-WT} and CD146^{LCK-KO} mice (representative of n = 3). (C) Analysis of apoptosis in DP cells from CD146^{LCK-WT} and CD146^{LCK-KO} mice. Right, percentages of apoptosis (n = 6 for WT or 5 for KO). (D) Analysis of apoptosis in isolated DP cells from CD146^{LCK-WT} and CD146^{LCK-KO} mice stimulated with the indicated concentration of anti-CD3/CD28 antibodies for 20 h (n = 3). (E) Relative expression of Nur77 mRNA in thymocytes from WT and KO mice (n = 3). (F) Percentages of BrdU⁺ cells in DP from WT and KO mice (n = 4). (G) Surface staining of CD146 in DP and CD4 thymocytes from OT-II^{tg}CD146^{CD4-WT} and OT-II^{tg}CD146^{CD4-KO} mice (representative of n = 3). Each symbol represents an individual mouse. One-way ANOVA followed by Bonferroni's correction (A) or two-tailed *t*-test (C, E, and F) or two-way ANOVA with multiple-comparison test (D) were performed. Data are shown as mean ± SEM; **p<0.01, ***p<0.001, n.s, not significant.

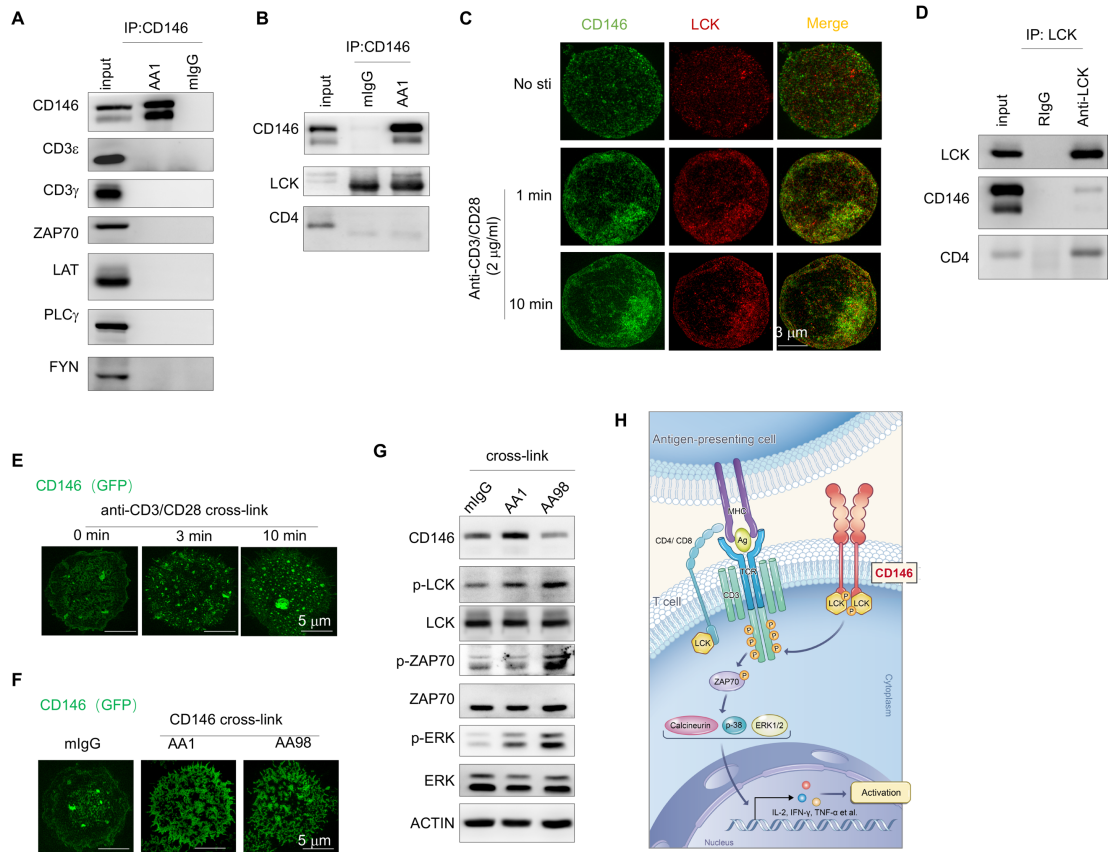


Supplementary Fig. 4. Impaired TCR-mediated response in CD146-deficient T cells. (A) Surface staining (left) of CD3 and CD8, CD19 on peripheral blood mononuclear cells (PBMC) from CD146^{WT} and CD146^{KO} mice. Numbers in the outlined areas indicate the percentages of each gate. Right panel, the percent of CD4 and CD8 populations in PBMC from CD146^{WT} and CD146^{KO} mice (n = 11). (B) Cell numbers of total PBMCs, CD4 and CD8 T cells, and non-T cells from WT and KO mice (n = 5). (C) CD69 expression on lymphoid CD4 and CD8 cells. Right, percent of CD69⁺ cells (n = 9). (D) Quantification of CD69⁺ cells in peripheral blood CD4 or CD8 cells from CD146^{WT} and CD146^{KO} mice (n = 9). (E) CD69 expression on naïve CD8⁺ T cells left stimulated for 5 h. Right top panel, quantification of CD69⁺ cells. Right bottom panel, quantification of CD69 MFI (n = 3). (F–G) Quantification of CD69⁺ cells in isolated CD4 or CD8 cells from CD146^{WT} and CD146^{LCK-KO} (F) or CD146^{CD4-KO} (G) splenic cells left unstimulated or activated with plate-bound anti-CD3/CD28 for 5 h (n = 3). (H) ELISA analysis of IL-2 or IFN- γ levels in culture supernatant of splenic naïve T cells after stimulation for 3d in vitro (n = 3). (I) FACS analysis of Granzyme B in CD8 T cells under anti-CD3/CD28 stimulation for 72 h (n = 3). (J) FACS analysis of CD146 expression on thymocyte DP, CD4, and CD8 cells (representative of n = 3).

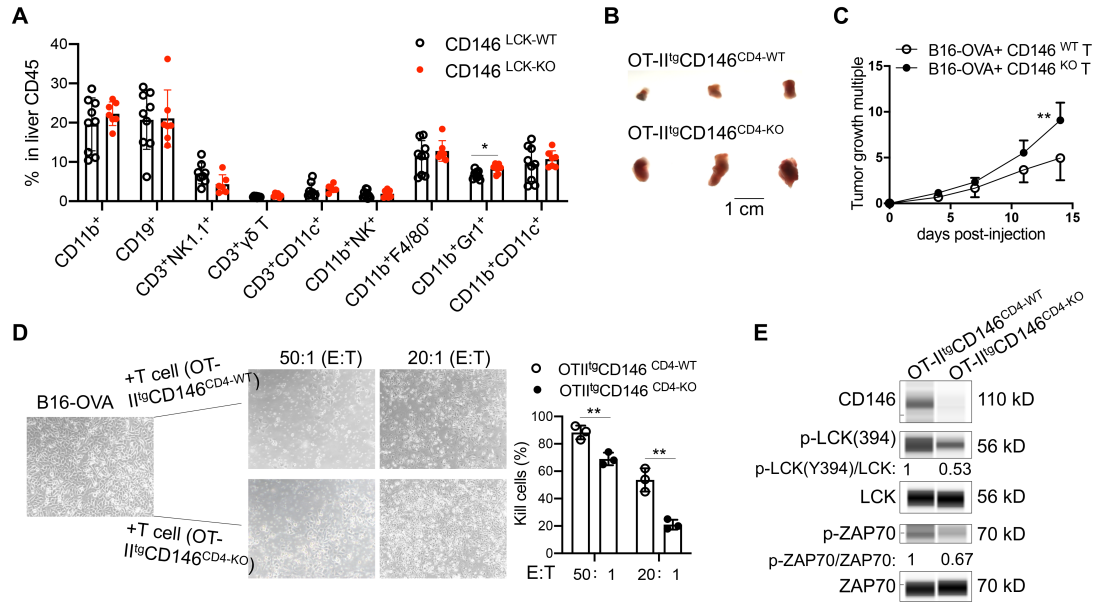
(K–L) Analysis of genes of *Cd146* (**K**), *Tnfa*, *Ifng* and *Il2* (**L**) in tamoxifen-treated splenic naïve T cells after stimulation for 24h. Each symbol represents an individual mouse. One-way ANOVA followed by Bonferroni's correction (**A–F**, **K**, **L**) or two-tailed *t*-test (**I**) were performed. Data are shown as mean ± SEM; **p* < 0.05, ***p* < 0.01, ****p* < 0.001.



Supplementary Fig. 5. Interruption of TCR signaling in CD146-deficient mice. (A) Calcium flux analysis in CD146^{WT} and CD146^{KO} splenic T cells stimulated with anti-CD3 and anti-CD28 antibodies. Arrows indicate the time of adding antibodies. Right, the quantification of MFI of Fluo-4 in CD4 and CD8 T cells (n = 3). **(B)** Immunoblot analysis of CD146, p-p38, and p-ERK in thymocytes stimulated with PMA/ionomycin for 5 min (representative of n = 3). Total p38, ERK1/2, and ACTIN served as loading controls. **(C)** Calcium flux analysis in CD146^{WT} and CD146^{KO} thymocytes stimulated with PMA/ionomycin. Arrows indicate when PMA/ionomycin was added. Right, the quantification of MFI of Fluo-4 (n = 3). **(D)** Surface staining of CD69 on isolated CD146^{WT} and CD146^{KO} splenic T cells stimulated with PMA/ionomycin at the indicated concentrations for 5 h. Right panel, the percentage quantification of CD69 MFI (n = 3). **(E)** Calcium flux analysis in CD146^{WT} and CD146^{KO} thymocytes stimulated with anti-CD3 antibody. Arrows indicate the time of adding antibody. Right, the quantification of MFI of Fluo-4 in DN, DP, CD4 SP and CD8 SP T cells (n = 6). **(F)** FACS analysis of CD146 expression on Jurkat cells after transfection of *CD146* shRNA or *CD146* plasmid (representative of n = 3). Each symbol represents an individual mouse. One-way ANOVA followed by Bonferroni's correction (**A**, **D**, and **E**) or two-tailed *t*-test (**C**) were performed. Data are shown as mean ± SEM; **p* < 0.05, ****p* < 0.001.



Supplementary Fig 6. CD146 interacts with LCK and acts as a platform to promote LCK activation. (A, B) Immunoblot analysis (IB) of CD146, CD3 ϵ , CD3 γ , ZAP70, LAT, PLC γ , FYN, LCK, and CD4 in Jurkat cells immunoprecipitated (IP) with anti-CD146 (AA1) or isotype IgG. (C) 3D-SIM (three-dimensional structured illumination microscopy) analysis of CD146 and LCK in Jurkat cells left unstimulated or stimulated with anti-CD3/CD28 antibodies for 1–10 min. (D) IB of LCK, CD146, and CD4 in Jurkat cells immunoprecipitated (IP) with anti-LCK. (E, F) Super-resolution imaging analysis of CD146-GFP in Jurkat cells cross-linked by anti-CD3/CD28 (E) or by anti-CD146 AA1 or AA98 (F). (G) IB of CD146, p-LCK (394), p-ZAP70, and p-ERK1/2 in Jurkat cells cross-linked by anti-CD146 antibodies AA1 or AA98 or control mIgG for 10 min. Total LCK, ZAP70, ERK1/2, β ACTIN or GAPDH served as the loading control. (H) Proposed model for the role of CD146 in TCR signaling. Upon TCR engagement, CD146 is recruited as a membrane component of TCR complex and dimerized. Dimerized CD146 promotes LCK activation, thus exerting a positive regulation on T cell activation. Data are representatives of three independent experiments.



Supplementary Fig. 7. CD146 on T cells enhances anti-tumor activity. (A) Percentage of infiltrated immune cells in liver CD45⁺ cells from DEN-induced HCC mice (n = 9 for WT or 7 for KO). (B) General view of B16-OVA tumors from OTII^{tg}CD146^{CD4-WT} or OTII^{tg}CD146^{CD4-KO} mice (representative of n = 3). (C) B16-OVA tumor growth in nude mice co-injected subcutaneously with B16-OVA cells and T cells (n = 5). (D) T cell-mediated tumor killing in vitro. E:T: T cells: tumor cells (n = 3). (E) Western immunoblot analysis of CD146, p-LCK (394), LCK, p-ZAP70 (319), and ZAP70 in splenic T cells isolated from tumor-bearing mice. Total LCK and ZAP70 proteins were included as loading controls (representative of n = 3). Each symbol represents an individual mouse (A) or one experiment (D). One-way ANOVA followed by Bonferroni's correction (A and D) or 2-way ANOVA with multiple-comparison test (C) were performed. Data are shown as mean ± SEM; *p < 0.05, **p < 0.01.

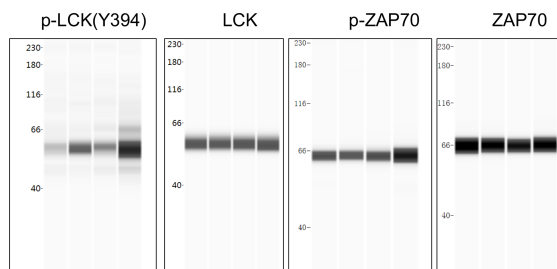
Table S1 CD146 shRNA used in Jurkat cell line for knockdown CD146.

| Name | Sequences | Respective cDNA locations |
|-----------------------|---------------------|---------------------------|
| CTR shRNA | Non-effective shRNA | Nonsense sequence |
| CD146 shRNA #1 | ATTCCTCAAGTCATCTGGT | 506–524 bp (190–196 aa) |
| CD146 shRNA #2 | GTTGAATCTGTCTTGTGAA | 1299–1318 bp (454–460 aa) |
| CD146 shRNA #3 | TGGCATTCAAGGAGAGGAA | 1342–1360 bp (468–474 aa) |
| CD146 shRNA #4 | GCTGGTTAAAGAAGACAAA | 634–652 bp (231–237 aa) |

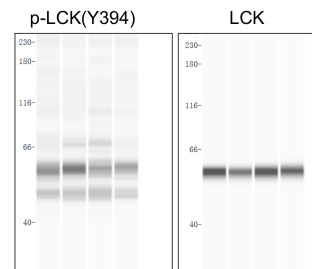
Table S2 Primers used in this study

| Gene name | Forward | Reverse |
|-------------------------|-------------------------|-------------------------|
| <i>Mcam-LoxP</i> | TGAAGTTCGGCTCAGGACAGAG | TGGGTCCTGAGAGCTTGGTG |
| <i>Cre</i> | CGATGCAACGAGTGATGAGG | CGCATAACCAGTGAAACAGC |
| <i>Cd146</i> | AGTCCTCACACCAGAGCCAA | CTCTTACGAGTCGGGGGCA |
| <i>Il2</i> | AGCATCATCTCAACAAGCCCT | AGCCCTTGGGGCTTACAAAA |
| <i>Cd69</i> | AGGCTTGTACGAGAAGTTGGA | AGTTCACCAGAATATCGCTTCAG |
| <i>Tnfa</i> | CCCAGGGACCTCTCTCTAATCA | AGCTGCCCTCAGCTTGAG |
| <i>Ifng</i> | ACGCTACACACTGCATCTTG | GTCACCATCCTTTTGCCAGTTC |
| <i>Nur77</i> | ATCCAAGTACAACGCACAGTACA | GCTTGGGTTTTGAAGGTAGCC |
| <i>Rpl13a</i> | GAGGTCGGGTGGAAGTACCA | TGCATCTTGGCCTTTTCCT |

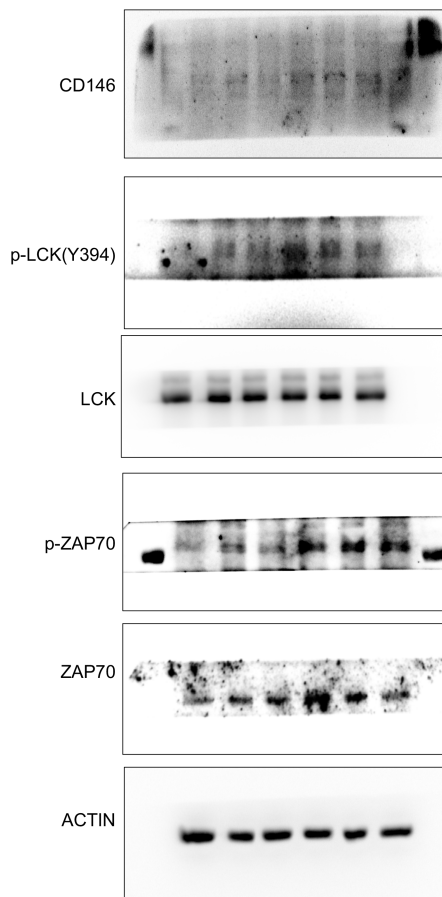
Full unedited gel for Figure 6A



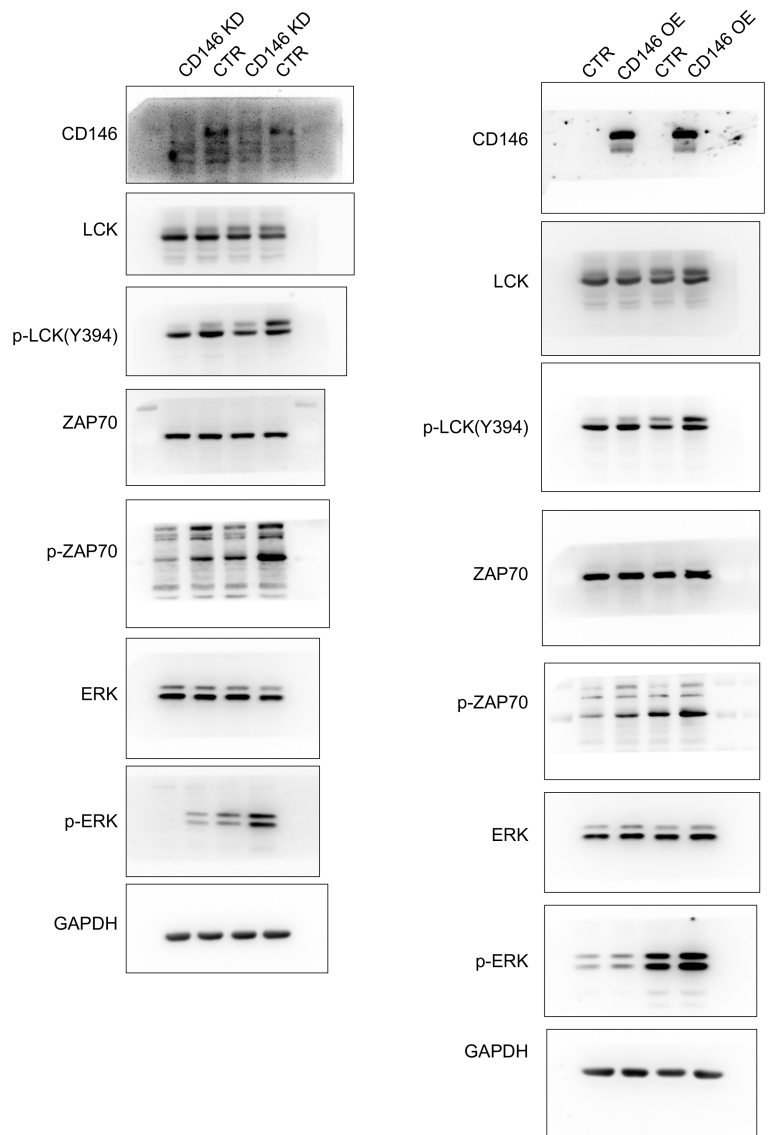
Full unedited gel for Figure 6E



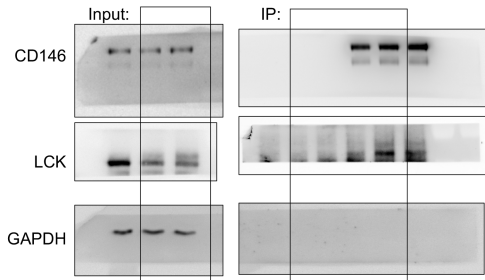
Full unedited gel for Figure 6D



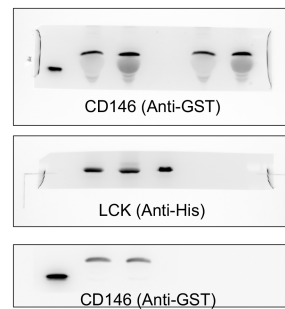
Full unedited gel for Figure 6G



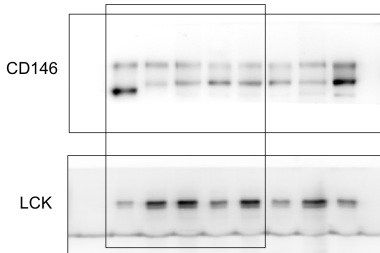
Full unedited gel for Figure 7A



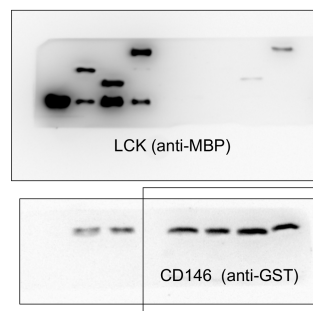
Full unedited gel for Figure 7C



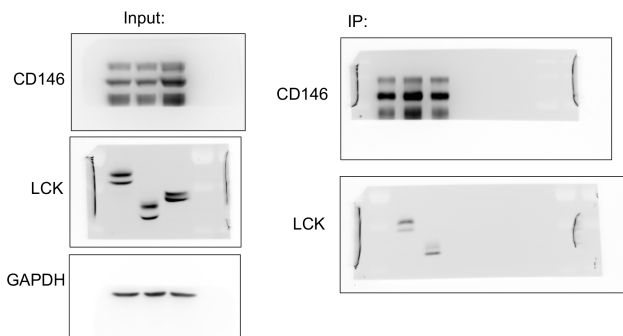
Full unedited gel for Figure 7E



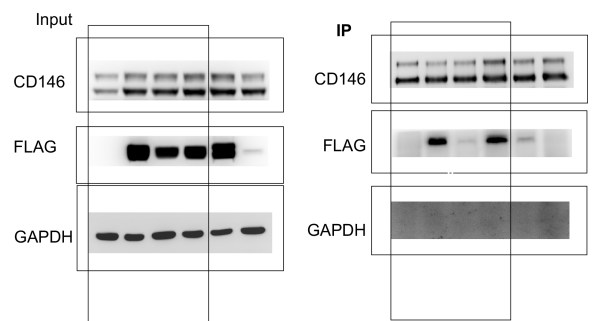
Full unedited gel for Figure 7H



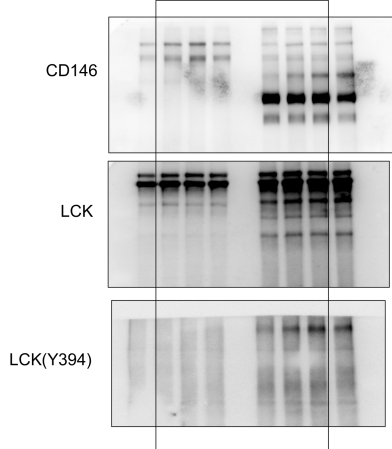
Full unedited gel for Figure 7I



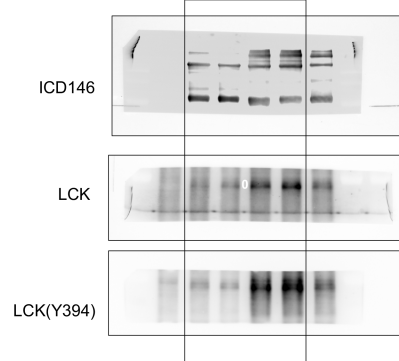
Full unedited gel for Figure 7J



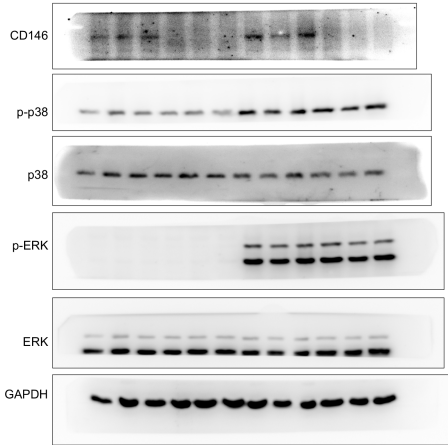
Full unedited gel for Figure 7K



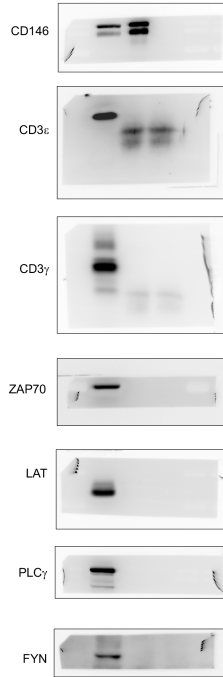
Full unedited gel for Figure 7N



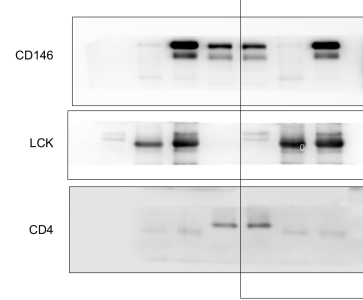
Full unedited gel for Sup Figure 5B



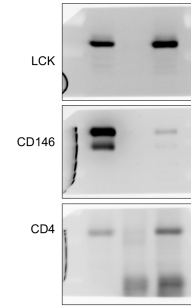
Full unedited gel for Sup Figure 6 A



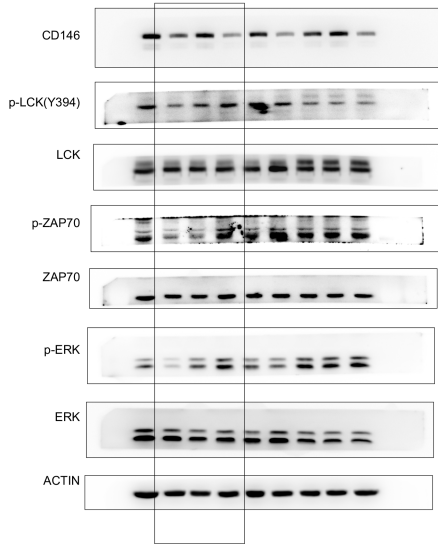
Full unedited gel for Sup Figure 6 B



Full unedited gel for Sup Figure 6 D



Full unedited gel for Sup Figure 6 G



Full unedited gel for Sup Figure 7E

